

# MITIGATING IDVC THERMAL DEFORMATION WITH MECHANICAL CONSTRAINT FOR RELIABLE ID MINIMUM GAP OPERATION\*

W. Li<sup>†</sup>, M. Qian, J. Liu, A. Donnelly, J. TerHAAR, Y. Piao, J. Xu  
Argonne National Laboratory, Lemont, IL, USA

## Abstract

Premature activation of the insertion device (ID) minimum-gap limit switches was observed during beamline commissioning at the Advanced Photon Source Upgrade (APSU). This was traced to vertical displacement of the insertion device vacuum chamber (IDVC), due to the temperature differences between the chamber and its strongback. Direct measurements of temperature and vertical displacement of the IDVC in a selected sector confirmed this effect, and simulations reproduced the underlying thermal deformation mechanism. To address this issue, we developed a simple mechanical constraint to limit the vertical displacement by adding an additional support stand. Post-installation tests successfully demonstrated its effectiveness, allowing the IDs to reach the minimum gap without activating the limit switches. This paper represents the investigation, simulation, and validation efforts to resolve this issue.

## INTRODUCTION

Hybrid Permanent Magnet Undulators (HPMUs) are essential components of the Advanced Photon Source Upgrade (APSU) for generating high-brightness X-ray beams for the insertion device (ID) beamlines. Insertion devices are designed with different period lengths and minimum gaps to cover specific X-ray energy ranges [1]. The minimum magnetic gaps of most IDs are designed to be 8.5 mm [2], while the insertion device vacuum chamber (IDVC) is designed with an outer height of  $7.5 \pm 0.3$  mm [3, 4], leaving a very small clearance on either side of the IDVC.

Due to these tight spacing constraints, the IDVC must be aligned within  $\pm 50$   $\mu\text{m}$  vertically and the chamber straightness maintained within  $\pm 100$   $\mu\text{m}$  throughout the 5.4 m full length [4]. To meet these tolerances, a strongback beam with the same length as the IDVC is designed to serve as both a support structure and an alignment reference. They connect via five L-brackets, each with three adjustment bolts, giving 15 correction points in total [4], as shown in Fig. 1.

Since the commissioning of the storage ring in 2024, the electron beam current increased, and commissioning of ID beamlines began. However, some IDs experienced premature activation of their minimum-gap limit switches at high beam current before reaching their designed minimum gaps. This discrepancy between the operational and the designed minimum gaps, referred to as the minimum gap shift, shown in Fig. 2. The shift varies across devices and can reach several hundred micrometers. For example, the upstream ID

(USID) in Sector 08 was limited to approximately 396  $\mu\text{m}$  above its designed minimum gap of 8.5 mm. These issues do not occur when the ring is not filled with beam. A systematic study of the minimum gap shift was conducted for all IDs with a 200 mA beam stored in the ring, shown in Fig. 2. It is observed that all the USIDs had their downstream-top (DST) switches activated, and all the downstream IDs (DSIDs) triggered their upstream-top (UST) switches. The only exception was one USID that exhibited activation of both its DST and upstream-bottom (USB) limit switches.

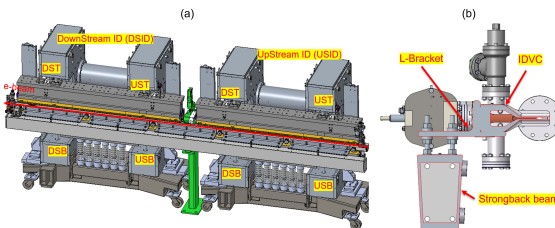


Figure 1: (a) Schematic of the IDVC and strongback in a sector with two IDs and an inline phase shifter. (b) Cross-sectional view of the IDVC mounted to the strongback.

Given the strong correlation of these events with beam current and that most activation events happened near the center of the IDVC, the most probable root cause is beam-induced thermal deformation of the IDVC. In this paper, we present our efforts investigating this issue and describe the solution developed to restore the operational minimum gaps for the IDs to the designed values.

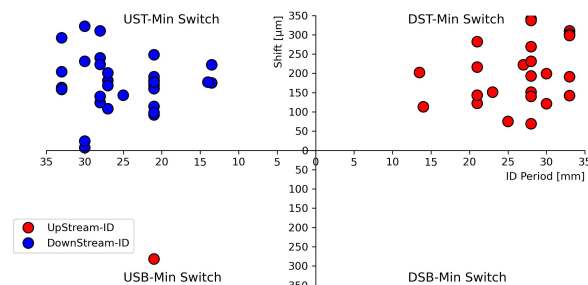


Figure 2: Minimum gap shifts relative to the designed values, measured with a 200-mA beam stored.

## MEASUREMENT

Thermocouples and a potentiometer were installed to directly measure temperature changes and IDVC vertical displacement. Eight high-precision thermocouples, with a resolution of 0.1 °C, were installed on the Sector 08 IDVC,

\* Work supported by U.S. Department of Energy, Office of Science, Office of Basic Energy Sciences, under Contract No. DE-AC02-06CH11357.  
† liw@anl.gov

its L-bracket, and strongback to monitor the temperature change at multiple locations. Vertical displacement is measured via a potentiometer on the inline phase shifter (ILPS) on the top-center of the IDVC, with a resolution of  $0.18 \mu\text{m}$ . These sensors were connected to MCC-DAQ units, and the real-time data were monitored and recorded via Ethernet.

The logged measurement data is shown in Fig. 3. It is observed that the IDVC cools down after the electron beam is dumped, and heats up again when the beam is injected and stored in the storage ring. During this period, the temperature of the strongback remains constant, indicating that the tunnel temperature is stable. Displacement measurements from the potentiometer show that the top surface of the IDVC moves downward as it cools, and moves upward as it heats up, consistent with thermally induced mechanical deformation. It should be noted that the approximately  $20\text{-}\mu\text{m}$  jump in the IDVC displacement around 8:00 AM was caused by the physical disengagement of the switch from the IDVC when the USID was opened from 9.0 mm.

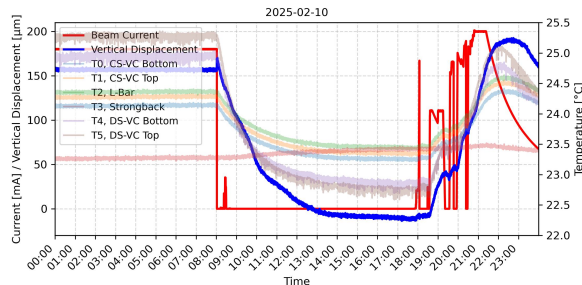


Figure 3: Measured beam current, IDVC vertical displacement, and temperature over 24 hours.

To quantify the thermal deformation, the average of the thermocouple readings on the top surface of the IDVC is used to present the average temperature of the IDVC. The difference between this average temperature and the strongback temperature is defined as  $\Delta T$ . It is observed that the IDVC displacement exhibits a linear relationship with  $\Delta T$ , yielding a slope of approximately  $90.7 \mu\text{m}/^\circ\text{C}$ . This result indicates that the deformation is proportional to the temperature gradient between the IDVC and its supporting strongback, confirming that the observed vertical displacement is predominantly driven by differential thermal expansion.

## SIMULATION

Based on the measurement data, a finite element thermal-structure analysis was performed. In the simulation setup, the strongback was fixed at the DS end, while the US end is allowed to move longitudinally, as described in [4]. The IDVC was mounted to the strongback using five L-brackets and secured with 15 nut screws. All components were modeled as rigidly bonded, with no slippage allowed between contact surfaces. A uniform temperature of  $24.5^\circ\text{C}$  was assigned to the IDVC and  $22.0^\circ\text{C}$  assigned to the strongback, resulting in a temperature difference of  $\Delta T = 2.5^\circ\text{C}$ , which closely matches the measurements.

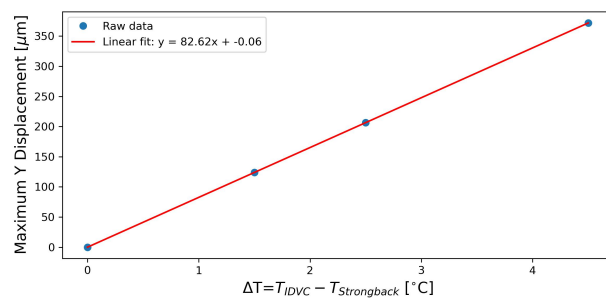


Figure 4: Maximum vertical displacement vs  $\Delta T$  according to simulation. The fitted slope is  $82.6 \mu\text{m}/^\circ\text{C}$ .

According to the simulation result, it is observed that the IDVC bends upward in the center, reaching a maximum vertical displacement of approximately  $206 \mu\text{m}$ . This displacement closely agrees with the potentiometer measurements, and agrees well with the previous observations that the activated switches are mostly located at the center top of the IDVC. By varying  $\Delta T$  in simulations, the corresponding maximum vertical displacements were calculated, as shown in Fig. 4. A linear relationship is observed, with a fitted slope of about  $82.6 \mu\text{m}/^\circ\text{C}$ , closely matching the measurements. This agreement validates the hypothesis that thermal deformation is proportional to the temperature differential.

It is observed that the strongback also undergoes a similar upward displacement, indicating that it is also lifted up due to the expansion of the IDVC. Although the strongback was designed to serve as the alignment reference, it is not rigid enough to withstand these thermal-induced stresses and therefore cannot maintain its straightness. The simulation also revealed a horizontal deformation of similar magnitude. Since the horizontal tolerance is larger, and this deformation does not impact the ID operations, it is not discussed further here.

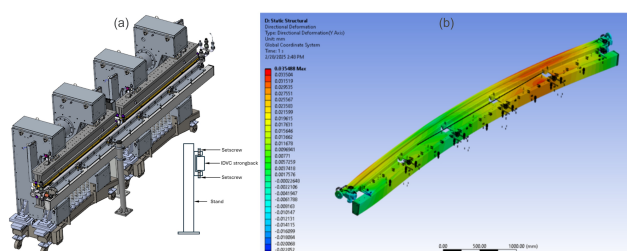


Figure 5: (a) Illustration of the proposed off-center support stand location. (b) Simulated vertical displacement with the support installed.  $\Delta T = 2.5^\circ\text{C}$ .

Given the excellent agreement between simulation and measurement, the temperature difference between the IDVC and the strongback seems to be the primary cause of the deformation; the two components deform together as a single unit. To eliminate the deformation, active compensation includes either heating up the strongback or cooling down the IDVC. However, such a system would require precise temperature sensing and real-time feedback control of the

heating or cooling load, making it relatively complex. As a simpler alternative solution, we proposed a mechanical solution: installing an additional support stand to hold the central part of the strongback to prevent its displacement, as well as the IDVC's.

This idea was tested in a simulation by applying a vertical constraint at the strongback center top to limit its displacement. The resulting maximum vertical IDVC displacement was significantly reduced to approximately 35  $\mu\text{m}$ , well within the alignment tolerance. The reaction force on the vertical constraint was about 444 N, which is practical for implementation. For ease of installation, an off-center support location, positioned in the gap between two L-brackets downstream, was also evaluated. As shown in Fig. 5, even when installed off-center, the support stand effectively suppressed the vertical deformation, keeping the displacement below 36  $\mu\text{m}$  across the entire vacuum chamber.

## INSTALLATION AND VALIDATION

To further validate the effectiveness of the proposed solution, support stands were installed in Sector 08 and Sector 20, as shown in Fig. 6. To maintain the vertical alignment of the IDVC during installation, a high-resolution laser displacement sensor (Keyence LK-G37) was used to precisely monitor the vertical variation of the IDVC position.



Figure 6: The additional stands installed to support the strongback in (a) Sector 08 and (b) Sector 20.

Experiments were conducted after the support stand was installed, and the vacuum chamber was elevated to a stable temperature. The beam current was ramped up to approximately 200 mA, and the IDs in Sector 08 and 20 were closed toward the design minimum gap of 8.5 mm to find out the achievable minimum gaps. The result is compared with the achievable minimum gaps measured before the support stands were installed, as shown in Table 1. Three out of these four IDs could reach the designed minimum gap without activating any limit switches. The only exception was the S08-USID, which triggered a minimum switch activated at 8.519 mm. It should be noted that the activated switch is located at the top of the upstream vacuum chamber, aligning well with the predicted IDVC deformation pattern as shown in Fig. 5, and it is below the maximum remaining in simulation. All these confirmed the effectiveness of the support stand solution in mitigating the IDVC deformation and restoring the intended ID operation range.

Additional confirmation was obtained from temperature and displacement monitoring in Sector 08 using thermocouples and potentiometers. Figure 7 shows the measurements

after the support stand was installed. Compared with measurements in Fig. 3, a larger temperature difference between the strongback and IDVC is observed in post-installation data, this is likely due to a higher beam current and/or a different filling pattern. Despite the larger temperature difference, the vertical displacement of the IDVC was significantly reduced after the support stand installation, with variations constrained to approximately 20  $\mu\text{m}$ .

Table 1: Comparison of achievable minimum gaps for IDs in S08 and S20 before and after the support stand was installed. Tests were done after several hours of operation with 200 mA. The triggered limit switch location is shown in parentheses.

| Device   | Before         | After          |
|----------|----------------|----------------|
| S08-USID | 8.782 mm (DST) | 8.519 mm (UST) |
| S08-DSID | 8.614 mm (UST) | 8.500 mm (N/A) |
| S20-USID | 8.643 mm (DST) | 8.500 mm (N/A) |
| S20-DSID | 8.661 mm (UST) | 8.500 mm (N/A) |

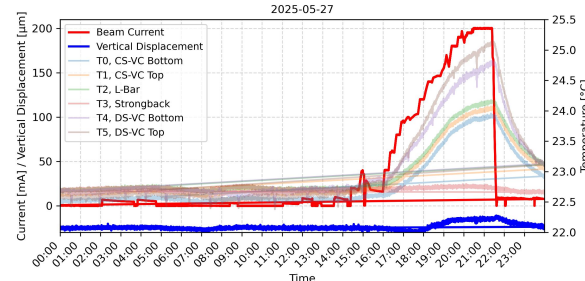


Figure 7: IDVC vertical displacement and temperature in Sector 08 after support stand installation.

## SUMMARY AND DISCUSSION

Maintaining micrometer-level mechanical stability poses a significant challenge, especially for long structures like the ID vacuum chamber at APSU, which spans 5.4 meters and features a 7.2-mm-thick nose. In this work, we resolved the issue of vertical displacement in the IDVC through a straightforward mechanical solution. The study also highlights the importance of accounting for potential thermal gradients between mechanically coupled components, such as the IDVC and its strongback, early in the design process. A carefully designed thermal management strategy would be essential to minimize temperature differentials and maintain structural stability. Even small temperature differences can cause measurable deformation, which is critical for systems like the IDVC, where the spatial clearance for ID limit switches is extremely small at the designed minimum gap.

## ACKNOWLEDGMENT

We would like to acknowledge the engineers and technicians for their valuable efforts in installing the support stands and assisting with the relocation of some thermocouples. We would like to acknowledge Bill Jansma for surveying the IDVCs and Roger Dejus for useful discussions.

## REFERENCES

- [1] R. Dejus *et al.*, “Status of undulators for the APS upgrade”, in *Proc. IPAC’24*, Nashville, TN, USA, May 2024, pp. 1376–1378.  
doi:10.18429/JACoW-IPAC2024-TUPG56
- [2] W. Li *et al.*, “New insertion device control system for the APS upgrade”, in *Proc. IPAC’24*, Nashville, TN, USA, May 2024, pp. 1394–1397.  
doi:10.18429/JACoW-IPAC2024-TUPG61
- [3] T. Fornek, *Advanced Photon Source Upgrade Project Final Design Report*, ANL, Lemont, IL, USA, Rep. APSU-2.01-RPT-003, May 2019. doi:10.2172/1543138
- [4] J. E. Lerch *et al.*, “APS upgrade insertion device vacuum chamber design”, in *Proc. NAPAC’19*, Lansing, MI, USA, Sep. 2019, pp. 450–452.  
doi:10.18429/JACoW-NAPAC2019-TUPLS02